AD-A107 686 ROCKWELL INTERNATIONAL THOUSAND OAKS CA ELECTRONICS--ETC F/G 20/
RESEARCH IN LPE OF DOPED LINBO3 AND LITAO3 THIN FILMS.(U)
JUN 81 R R NEURGAONKAR F49620-77-C-0081
UNCLASSIFIED ERC41004.11FR AFOSR-TR-81-0721 NL

1 of 1
ADA
107686

END
DATE FILMED
11-81
DTIC

LEVEL I

ERC41004.11FR

Copy No. 16

ERC41004.11FR

RESEARCH IN LPE OF DOPED $LiNbO_3$ AND $LiTaO_3$ THIN FILMS

FINAL REPORT FOR THE PERIOD
April 1, 1977 through March 31, 1981

GENERAL ORDER NO. 41004
CONTRACT NO. F49620-77-C-0081

Prepared for

Air Force Office of Scientific Research
Building 410
Bolling Air Force Base
Washington, DC 20332

R. Neurgaonkar

Principal Investigator

JUNE 1981

Rockwell International
Microelectronics Research and
Development Center

Approved for public release;
distribution unlimited.

UNCLASSIFIED

SECURITY CLASSIFICATION OF THIS PAGE (When Data Entered)

REPORT DOCUMENTATION PAGE	READ INSTRUCTIONS BEFORE COMPLETING FORM
1. REPORT NUMBER AFOSR-TR-81-0721	2. GOVT ACCESSION NO. AD-A107 859	3. RECIPIENT'S CATALOG NUMBER
4. TITLE (and Subtitle) Research in LPE of Doped $LiNbO_3$ and $LiTaO_3$ Thin Films	5. TYPE OF REPORT & PERIOD COVERED Final Report 04/01/77 through 03/31/81
	6. PERFORMING ORG. REPORT NUMBER ERC41004.11FR
7. AUTHOR(s) R. Neurgaonkar	8. CONTRACT OR GRANT NUMBER(s) F49620-77-C-0081
9. PERFORMING ORGANIZATION NAME AND ADDRESS Rockwell International Microelectronics Research and Development Center; 1049 Camino Dos Rios Thousand Oaks, CA 91360	10. PROGRAM ELEMENT, PROJECT, TASK AREA & WORK UNIT NUMBERS 2306/B1 61102F
11. CONTROLLING OFFICE NAME AND ADDRESS Air Force Office of Scientific Research Building 410 Bolling Air Force Base, DC 20332	12. REPORT DATE June 1981
	13. NUMBER OF PAGES 53
14. MONITORING AGENCY NAME & ADDRESS(if different from Controlling Office)	15. SECURITY CLASS. (of this report) Unclassified
	15a. DECLASSIFICATION/DOWNGRADING SCHEDULE

16. DISTRIBUTION STATEMENT (of this Report)

Approved for public release; distribution unlimited

17. DISTRIBUTION STATEMENT (of the abstract entered in Block 20, if different from Report)

18. SUPPLEMENTARY NOTES

19. KEY WORDS (Continue on reverse side if necessary and identify by block number)

Lithium niobate, lithium tantalate, liquid phase epitaxy, surface acoustic wave, temperature stability

20. ABSTRACT (Continue on reverse side if necessary and identify by block number)

The crystal chemistry approach has been shown to be successful in improving the temperature stability of ferroelectric $LiNbO_3$ phase. $LiNbO_3$ films doped with Na^+, $Na^+ + Ta^{5+}$, $Co^{2+} + Zr^{4+}$ etc. have successfully been grown by the LPE technique using the vanadium containing flux systems. X-ray diffraction studies indicate that the films grown from the vanadium containing fluxes have a high single crystallinity with good epitaxy. To date, the temperature coefficient of SAW velocity was reduced by 40%; this translates into 40%

DD FORM 1 JAN 73 1473 EDITION OF 1 NOV 65 IS OBSOLETE

UNCLASSIFIED

SECURITY CLASSIFICATION OF THIS PAGE (When Data Entered)

improvement in the temperature stability of $LiNbO_3$ SAW devices. This is a significant result in the present work and opens a new interest in the $LiNbO_3$ family for SAW application.

TABLE OF CONTENTS

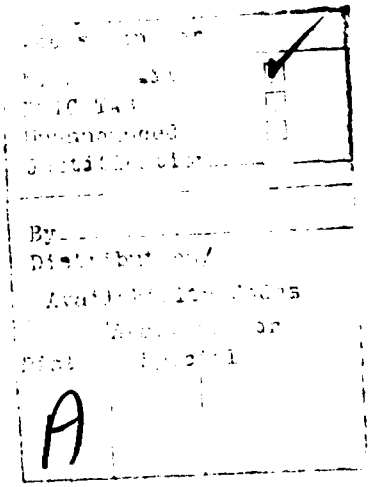

LIST OF FIGURES

LIST OF FIGURES

LIST OF TABLES

FOREWORD

This report was prepared by Dr. R.R. Neurgaonkar, Principal Investigator, under contact No. F49620-77-C-0081, Project 2306/B1. It covers the period April 1, 1977 to March 1981 and is the final report for this contract. The work described herein was carried out by the Rockwell International/Microelectronics Research and Development Center in Thousand Oaks, California.

ABSTRACT

The crystal chemical approach has been shown to be successful in improving the temperature stability of ferroelectric $LiNbO_3$ phase. $LiNbO_3$ films doped with cations that are larger than Li^+ and Nb^{5+}, e.g., Na^+, $Na^+ + Ta^{5+}$, Ag^+, $Co^{2+} + Zr^{4+}$, etc., have successfully been grown by the liquid phase epitaxial (LPE) technique using the vanadium containing flux systems. X-ray diffraction studies indicate that the films grown from the vanadium containing fluxes have a high single crystallinity with good epitxy.

To date, the temperature coefficient of SAW velocity was reduced by 40%; this translates into 40% improvement in the temperature stability of $LiNbO_3$ SAW devices. this is a significant result in the present work and opens a new interest in the $LiNbO_3$ family for SAW application. By using such a novel approach, it should be possible to improve the temperature stability of other important structural families such as quartz or tungsten bronze structural family compositions.

1.0 INTRODUCTION

Early successful use of liquid phase epitaxy (LPE) in the preparation of Ge tunnel diodes and GaAs laser diodes stimulated great scientific interest on the part of numerous investigators to adapt the liquid phase epitaxial process to a wide variety of materials and devices. As a consequence, the liquid phase epitaxial (LPE) method has displaced several other synthesis techniques for the preparation of epitaxial films for several important devices and is considered a basic useful tool of solid-state technology.

Liquid phase epitaxy is most widely used today for the preparation of epi-films of important materials such as semiconductor GaP, GaAs, (GaAl)As, etc., as well as magnetic bubble garnets because of some unique advantages of liquid phase epitaxy over the vapor phase epitaxy method.[1-11] In general, LPE is advantageous because of the fact that: (1) the equipment used for this work is much simpler than that required for VPE; (2) higher deposition rates can be easily achieved, thus allowing the growth of thick epitaxial layers in convenient time periods, and (3) the choice of dopants for LPE is wider than for VPE and unusual properties can be achieved in some cases because of stoichiometric differences. The limitation of the LPE technique is severe when the substrate and the epilayer have dissimilar lattice constants. The growth of epi-films in such cases is very difficult and films often crack.

The work on the liquid phase epitaxy for the acoustic-surface-wave project was initiated at Rockwell with the specific objective of developing a superior material for surface acoustic wave devices. These SAW devices are

very important and are commonly used to solve the problems in the technological areas of bandpass filters, resonators, oscillators, and discriminators. All these devices are, however, limited in their performance by the surface acoustic wave (SAW) materials availability. At the present time, three main SAW materials, namely, quartz, $LiTaO_3$ and $LiNbO_3$ are being used for this purpose. Very recently, the growth of $LiNbO_3$ thin films by the LPE method has been reported.[12-15] These films were grown with an aim to study the electro-optic properties; however, nothing is known about their use for SAW applications. Furthermore, there was no information available on how to alter the physical properties of $LiNbO_3$. During last four years we conducted a systematic study of LPE of pure and modified $LiNbO_3$ and $LiTaO_3$ on $LiNbO_3$ substrates, and evaluated the effect of such substitutions on physical properties, especially temperature coefficient of surface wave velocity. Based on our current results the Na^+-modified $LiNbO_3$ films, demonstrated that this technique offers an attractive opportunity to produce improved materials for SAW devices. It should be mentioned here that this is the first time such a technique is being exploited and developed for SAW application.

To date, the temperature coefficient of surface wave velocity has been reduced by 40%. This is translated into a 40% improvement in the temperature stability of $LiNbO_3$ SAW devices. $LiNbO_3$ SAW filters are important elements to such DoD systems as radar, communication and navigation equipment.

2.0 PROGRESS FROM 1977 TO 1981

During the past four years our efforts were concentrated on the growth of modified films of $LiNbO_3$ on $LiNbO_3$ substrates. The objective was to verify the hypothesis that by doping films one can achieve control of key acoustic device parameters. The specific goal of this work was to demonstrate this approach by the lowering of the temperature coefficient of surface wave velocity. Sodium modified films were grown and the concept was verified by an experimentally observed 40% reduction in the temperature coefficient of surface wave velocity. The results of this research have already been reported in the Journal of Applied Physics, Journal of Crystal Growth, the Annual Frequency Control and Ultrasonic Symposiums, and Met. Res. Bull.

An overall view of the important activities of this project and their interrelationship is shown in Fig. 1. Progress in each area was accomplished and is discussed in detail in the subsections of this report. The design and fabrication of growth equipment used in our research was accomplished and is covered in detail in Section 3.1. Initial solvents used in the film growth were dictated by such macroscopic qualities as absence of cracking and film texture. Solvent selection and experimental growth experiments for doped films is discussed in Sections 3.4.1 through 3.4.2. Our initial attempt to grow films resulted in substrate cracking and, in general poor film quality. Improvements in the growth apparatus and flux composition resulted in the ability to grow excellent films on substrates as large as 5 cm.

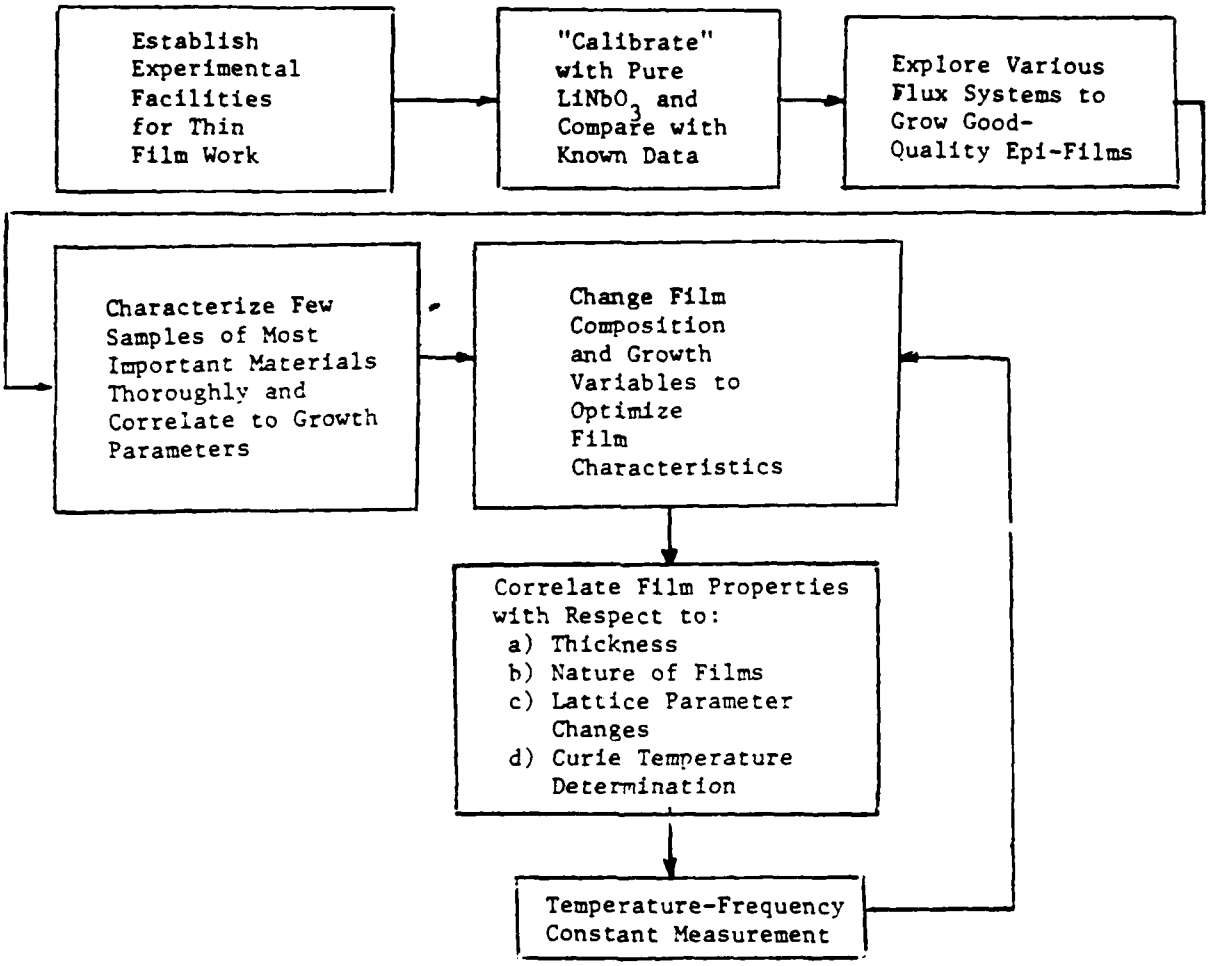

Fig. 1 Flow chart of activities.

Characterization of the doped and undoped films was performed in several different experiments and is discussed in Section 3.5 Optical and electron beam microscopy revealed the film's texture and provided a coarse evaluation of film quality. X-ray diffraction analysis and a determination of the Curie temperature resulted in considerably more data regarding the internal quality of the films grown.

The temperature coefficient of surface wave velocity was determined by fabricating a high Q surface wave resonator on the film/substrate. Measurement of the resonant frequency of this device as the temperature as varied provided the data necessary to evaluate the temperature coefficient. To date, the best result observed by this method was been a temperature coefficient of -56 ppm/°C or a reduction of approximately 40% from that of pure $LiNbO_3$.

3.0 LPE GROWTH OF MODIFIED $LiNbO_3$ FILMS

3.1 Experimental Background

Ferroelectric $LiNbO_3$ and $LiTaO_3$ are isostructural and belong to the ilmenite structural family (R3C). Although the ionic size of Nb^{5+} and Ta^{5+} (0.78 Å) is similar, the unit cell dimensions are slightly different. When Nb^{5+} was replaced withTa^{5+} in the $LiNbO_3$ structure, the unit cell a_A increased from 5.148 Å to 5.152 Å and the unit cell c_A reduced from 13.863 Å to 13.786 Å. These small changes in the unit cell dimensions appear to be associated with significant reduction in the temperature coefficient of the SAW velocity, i.e., from 90 ppm/°C for $LiNbO_3$ to 35 ppm/°C for $LiTaO_3$; the ferroelectric phase transition temperature was also reduced from 1200°C for $LiNbO_3$ to 660°C for $LiTaO_3$. This strongly suggests that the temperature coefficient of SAW velocity should reduce if the unit cell a_A is increased and the unit cell c_A is decreased for modified $LiNbO_3$. Based on our extensive crystal chemistry work and previous liquid phase epitaxial work on the $LiNbO_3$ family compounds, this can be accomplished for $LiNbO_3$ films under the following two conditions:

1. Use of excess of Nb^{5+} in the modified $LiNbO_3$ films; this can be accomplished by using the Li^+ - free flux systems such as, K_2WO_4, KVO_3, K_2MoO_4, BaV_2O_6 and $NAVO_3$ etc.

2 Use of large cations of Li^+, Nb^{5+} or for both in the $LiNbO_3$ phase.

According to our crystal chemistry work,[16-18] large cations for Li^+ and Nb^{5+} tend to increase the unit cell a_A and reduce the unit cell c_A, and vise versa; hence as summarized in Table 1 various large cations have been tried in the present LPE growth work.

Table 1

Cations That are Substituted in $LiNbO_3$ Films

System	Li-Site 0.88 A	Nb^{5+}-Site 0.78 A	Ionic Size A	Crystalline Solubility	Reference
$LiNbO_3:Nb^{5+}$	-	Nb^{5+}	0.78	Limited	Ballman
$Li_{1-x}Na_xNbO_3$	Na^+	-	1.16	7 mole%	Present Work
$Li_{1-x}Ag_xNbO_3$	Ag^+	-	1.29	5 mole%	Present Work
$Li_{1-x}Co_xNb_{1-x}Zr_xO_3$	Co^{2+}	Zr^{4+}	0.87*	30 mole%	Present Work
$Li_{1-x}Ca_xNb_{1-x}Zr_xO_3$	Ca^{2+}	Zr^{4+}	1.0*	20 mole%	Present Work
$Li_{1-x}Ca_xNb_{1-x}Ti_xO_3$	Ca^{2+}	Ti^{4+}	0.94*	15 mole%	Present Work
$Li_{1-x}Na_xNb_{1-y}Ta_yO_3$	Na^+	Ta^{5+}	0.96*	Extensive	Present Work

*Indicate average ionic size for the given combination.

3.2 Growth Apparatus

Our current growth setup consists of a vertical platinum-wound resistance furnace capable of reaching 1500°C which is manufactured by W.P. Keith and Co. It has an overall length of 20 in. with 2-1/2 in. internal

diameter and external shunts at 2-in. intervals for adjusting the temperature profile. A temperature control system consisting of an Eurotherm Model No. 919 digital-high stability controller capable of ±0.2°C, an Eurotherm Model No. 931 SCR power supply assembly, and an Eurotherm Model No. 125 digital temperature programmer, ramping up or down, from 0.1 to 10°C/min. Growth temperature has been carefully monitored by placing two 90%-10% Pt-Rh thermocouples, one inside and the other outside of the melt. This apparatus also includes a substrate preheating furnace (600-700°C), located above the growth chamber, which isolates the substrate from any undesirable vapor during a preheating period. This precaution is particularly necessary when the substrate is held on a heavy, high-heat-capacity platinum disk.

A number of suitable designs for achieving the lowering or raising of the substrate have been employed and a lead-screw arrangement was chosen for the present growth experiments. This arrangement is mainly used to lower or raise the substrate assembly holder through a predetermined distance from the top of the furnace to the appropriate immersion depth in the melt, or from the melt to the top of the furnace. Precise positioning is maintained by adjusting a limit-switch in both directions. This system is capable of traveling as slow as one inch per 20 min up or down, and rotating at 0.1 rps to 10 rps. Slow speed raising or lowering is essential in the present study to eliminate cracking of substrates due to thermal shock.

3.3 Substrate Preparation and Growth Procedure

Substrates of the desired material (usually Y-cut $LiNbO_3$) have been carefully prepared and cleaned before and after the growth experiments. Each substrate piece (about 0.5 cm wide and 3 to 5 cm long) is first rinsed thoroughly in acetone and isopropyl alcohol to remove contaminates, then cleaned in water. A non-abrasive soap solution is used to clean the surface completely and then dipped in dilute HF acid. The substrate is then rinsed again with water and is blown dry with filtered nitrogen gas. The substrate is now carefully mounted onto the ceramic holder by platinum wire through a hole in the substrate. The holder is then slowly lowered into the hot zone and is kept above the melt about 30 min before it is immersed. The results of this study indicate that the growth of the thin film can be achieved by dipping the substrate either vertically or horizontally into the melt. Y and Z-cut $LiNbO_3$ substrates were used and growth rate of epi-films was controlled by changing the temperature and growth time. After the successful growth, thin films were carefully leveled and then cleaned in dilute HCl. The films thus prepared were of excellent quality and desired thickness.

3.4 Solvents and Film Growth

Crucial to the success of this isothermal growth is an ability to supercool the solution without the occurrance of spontaneous nucleation. It is therefore necessary, before LPE can be performed, to find a suitable flux (solvent) for each modified $LiNbO_3$ composition. Although a large number of solvents have been identified for this family, the choice in the present work

is restricted to only the vanadium-containing solvent because of the following important reasons:

1. V^{5+} cation has a strong preference for the 4-fold coordinated site and, hence, no vanadium inclusion in the $LiNbO_3$ structure is observed.

2. Supercooling range for the V^{5+}-containing solvents is reasonably high, of an order of 20° to 40°C.

3. V^{5+}-containing solvents melt at significantly low temperatures, and thus allowed LPE growth at much lower temperatures.

4. All V^{5+}-containing solvents dissolve in water or dil. acids, and cleaning of films therefore posed no problems in the present work.

Before any liquid phase epitaxial technique was applied for film growth, all the systems of interest, e.g., KVO_3-$LiNbO_3$, $NaVO_3$-$LiNbO_3$, $LiVO_3$-$LiNbO_3$, $Li_{1-x}Na_xVO_3$-$LiNbO_3$, $LiVO_3$-$Li_{1-x}Co_xNb_{1-x}Zr_xO_3$, $Li_{1-x}Na_xVO_3$-$LiNb_{1-y}Ta_yO_3$, and $LiVO_3Li_{1-x}Ca_xNb_{1-x}Zr_xO_3$ etc. were investigated, and temperature and compositional boundaries over which modified $LiNbO_3$ cristallizes were established by x-ray powder diffraction and DTA techniques. The results of this investigation are summarized in the following sections.

3.4.1 Simple Substituted $LiNbO_3$ Films

An examination of the phase diagram in Figs. 2a -2c shows that the $LiNbO_3$ phase crystallizes in all three systems when the concentration of $LiNbO_3$ is above 50 mole% and, hence, the dipping temperature had to be in the 1100°C to 1150°C range. LPE growth of the Nb^{5+}-rich films was successful on the Y-cut $LiNbO_3$ substrates from the K_2WO_4-$LiNbO_3$ and KVO_3-$LiNbO_3$ systems, and the unit cell a_A changed from 5.148 A for the $LiNbO_3$ substrate to 5.153 A for the Nb^{5+}-rich $LiNbO_3$ films. Ballman et al[12] also studied the K_2WO_4-$LiNbO_3$, and the results of our investigations are in excellent agreement. According to our crystal chemical studies,[15,16] K^+ does not prefer the 6-fold coordinated Li^+-site in the $LiNbO_3$ structure; the changes in the unit cell a_A are therefore considered to be due to changes in the Li:Nb ratio.

In the third system $NaVO_3$-$LiNbO_3$, the situation is completely different. The crystal chemistry work shows that about 7 mole% sodium dissolves in the $LiNbO_3$ structure and, for this addition of sodium, the unit cell a_A changed from 5.148 A for $LiNbO_3$ to 5.179 A for $Li_{0.93}Na_{0.07}NbO_3$. This created a large lattice mismatch between the $LiNbO_3$ or $LiTaO_3$ substrate and the film, and the LPE growth was therefore unsuccessful.

Since the Na^+-modified $LiNbO_3$ films are of significant interest in the present work, the lithium concentration in the charge was increased, and the system was studied on the tenary assemblage as $NaVO_3$-$LiVO_3$-$LiNbO_3$. As shown in Fig. 3, the Na^+-modified $LiNbO_3$ solid solution extends over a wide compositional range. The compositions represented on the binary joins in

ERC80-7552

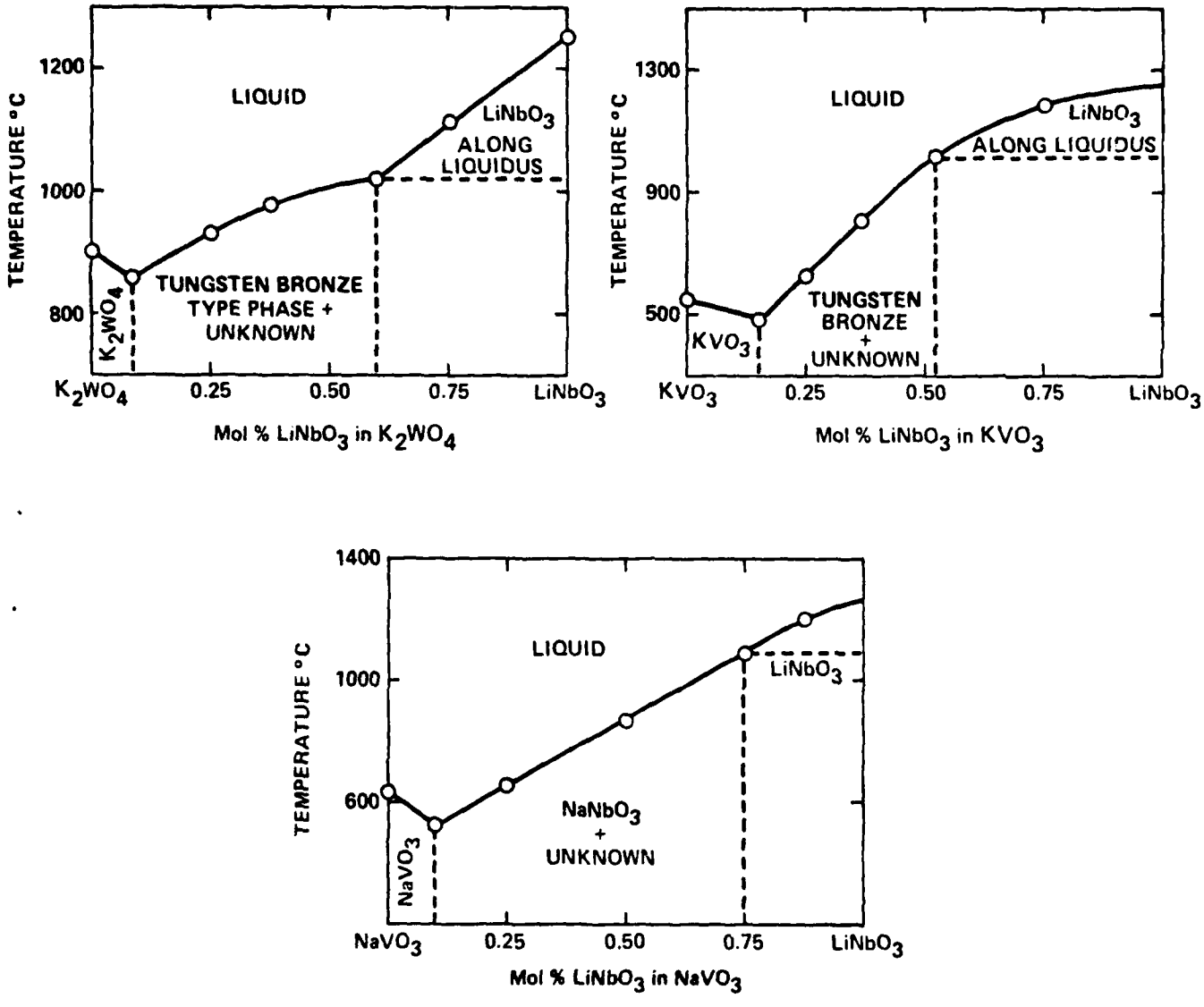

Fig. 2 Partial phase diagrams: (a) K_2WO_4-$LiNbO_3$, (b) KVO_3-$LiNbO_3$ (c) $NaVO_3$-$LiNbO_3$.

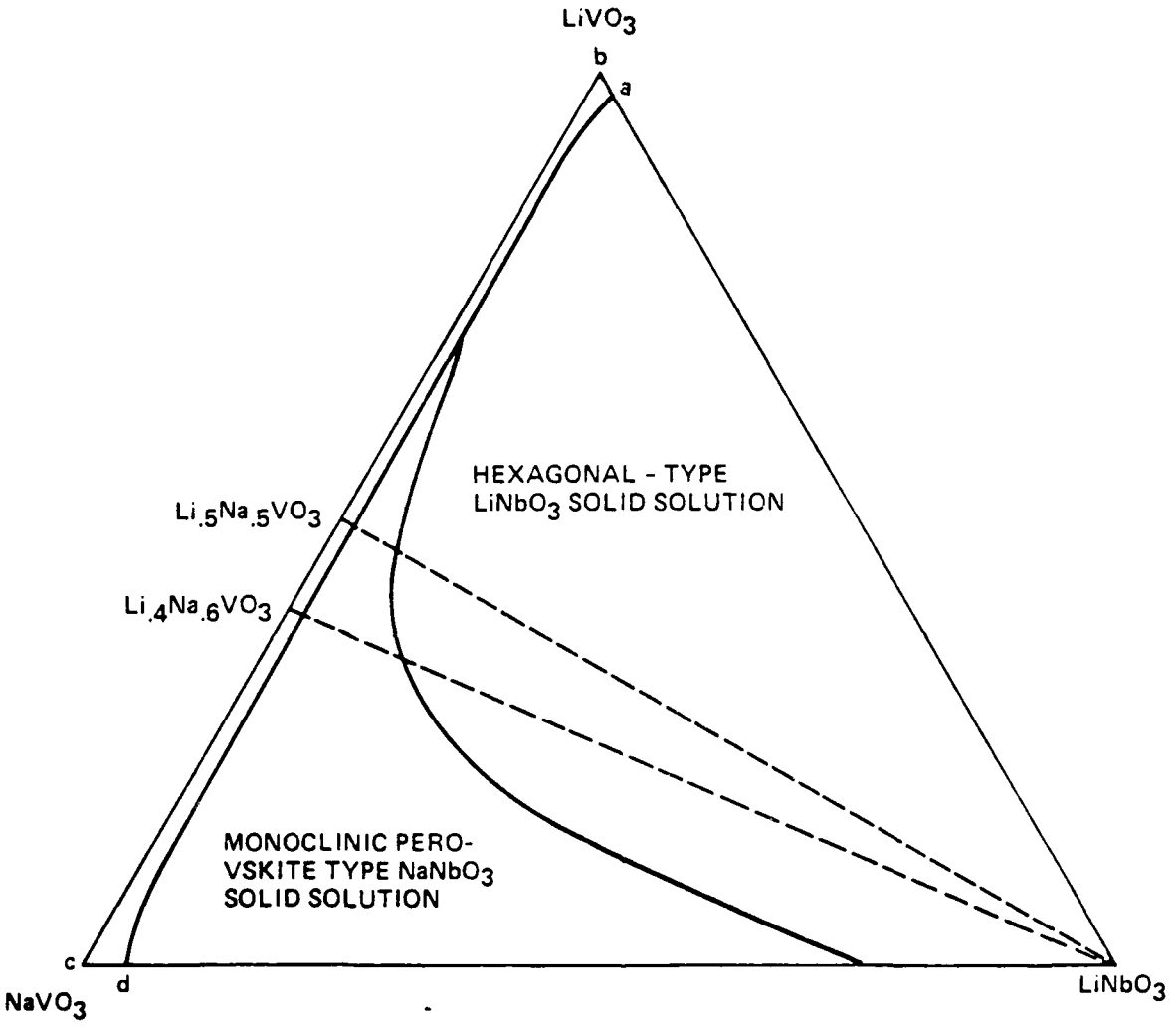

Fig. 3 System $NaVO_3$-$LiVO_3$-$LiNbO_3$, in air, at 1000°C.

Fig. 3 as $Li_{0.5}Na_{0.5}VO_3$-$LiNbO_3$ and $Li_{0.4}Na_{0.6}VO_3$-$LiNbO_3$ were studied in detail. It has been shown that the unit cell a_A increases with increasing concentration of sodium in both the binary systems. As shown in Fig. 4, the unit cell a_A changed from 5.143 A for Li-rich $LiNbO_3$ (grown from $LiVO_3$ flux) to 5.156 A for the Na^+-modified $LiNbO_3$ phase. This results showed that, by using this assamblage, sodium concentration can be changed from 0 mole% to 2 mole% in the $LiNbO_3$ phase. This is an interesting and significant result in the present work and offers an excellent opportunity to grow Na^+-modified $LiNbO_3$ films. Since the system $Li_{0.4}Na_{0.6}VO_3$-$LiNbO_3$ contains about 2 mole% Na^+ in the $LiNbO_3$ phase, this mixture was employed for film growth experiments. An appropriate dipping temperature for this composition is about 800°C. The Y-cut $LiNbO_3$ substrate was used and films as thick as 40 to 60 μm could easily be grown. Figure 5 shows a typical cross section of Na^+-modified $LiNbO_3$ film grown on the Y-cut $LiNbO_3$. The new films have excellent quality and are smooth enough to fabricate SAW devices on them.

Ag^+-modified $LiNbO_3$ films were also grown by the same technique using the $Li_{0.54}Ag_{0.5}VO_3$ flux. Since the concentration of Ag^+ was very negligible in the films, it was found difficult to characterize Ag^+-modified $LiNbO_3$ films.

3.4.2 Charge-Coupled Substituted $LiNbO_3$ Films

As discussed in the previous section, since the substitution of sodium more than 1 mole% was difficult in the $LiNbO_3$ films, another ion such as Ta^{5+} was added in the $Li_{1-x}Na_xNb_{1-y}Ta_yO_3$ system to improve the temperature

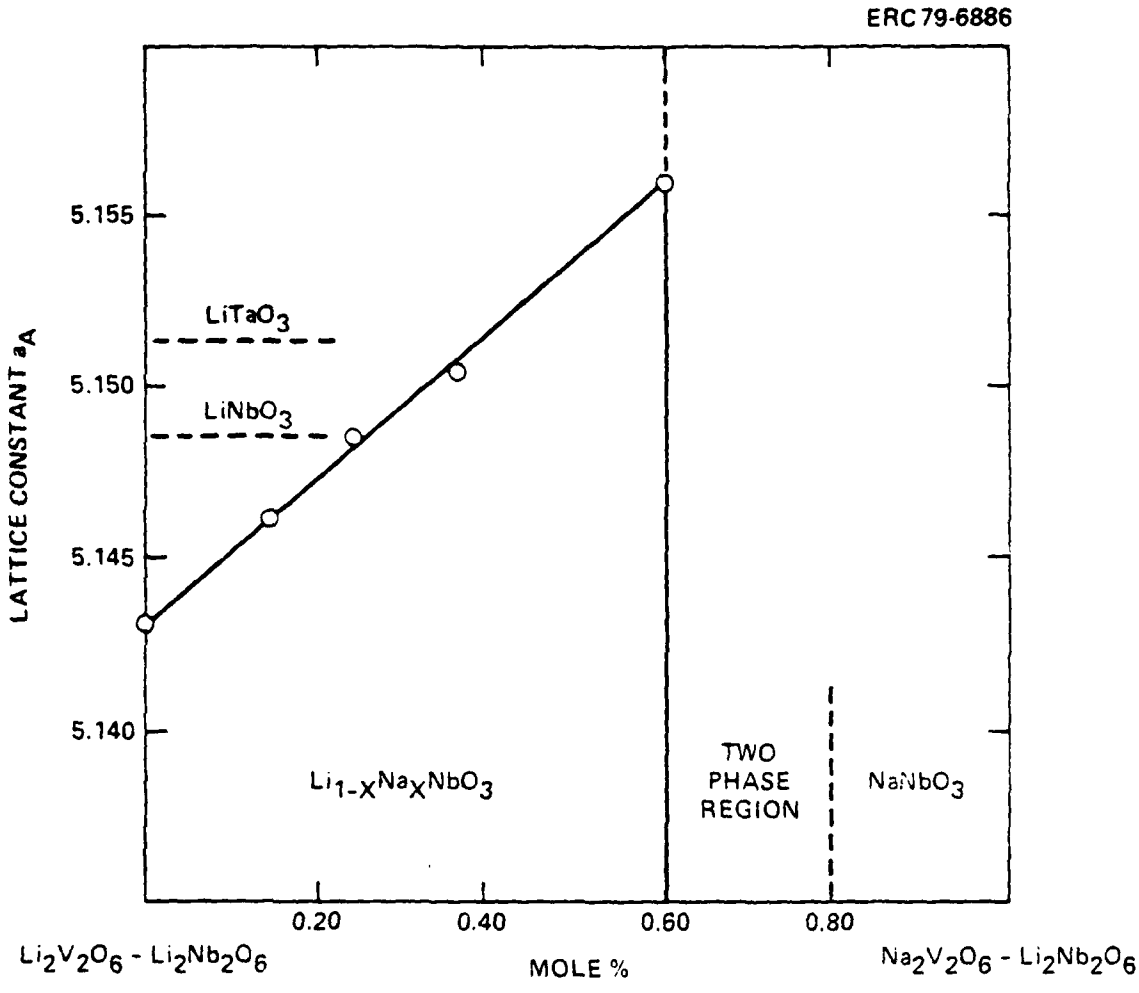

Fig. 4 Variation of the unit cell a_A for the $Li_{1-x}Na_xNbO_3$ system.

SC78-3045

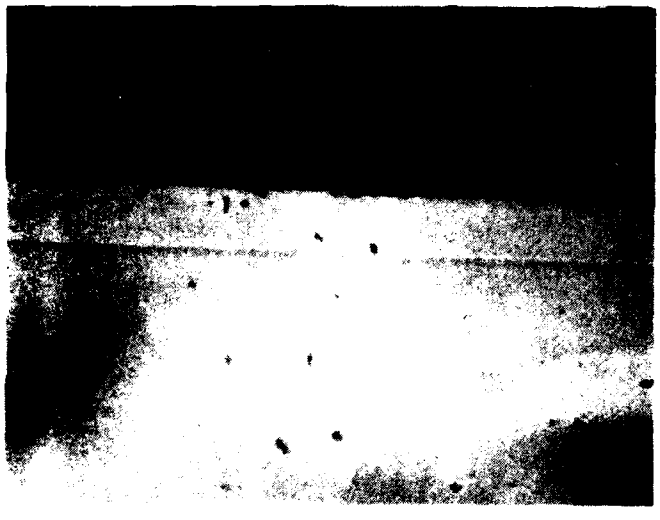

Fig. 5 A typical cross section of Na^+-containing $LiNbO_3$ film on the Y-cut $LiNbO_3$ substrate.

stability. The selection of tantalum was based on its ability to reduce the temperature coefficient of SAW velocity and because both the $LiNbO_3$ and $LiTaO_3$ phases form a complete solid solution.[19,20] As shown in Fig. 6, the ternary phase diagram for the $LiVO_3$-$NaVO_3$-$LiNb_{1-y}Ta_yO_3$ was established, and it has been shown that the modified $Li_{0.99}Na_{0.01}Nb_{1-y}Ta_yO_3$ phase extends over a wide compositional range. The determination of liquidus temperature for the two systems $Li_{0.4}Na_{0.6}VO_3$-$LiNb_{1-y}Ta_yO_3$ and $Li_{0.5}Na_{0.5}VO_3$-$LiNb_{1-y}Ta_yO_3$ showed that the addition of tantalum increased the dipping temperature substantially (over 1000°C). The appropriate dipping temperature for these systems was between 1100°-1250°C, depending upon the concentration of Ta^{5+} in the system. Initially, the LPE growth was carried out on the $LiNbO_3$ substrate and found unsuccessful; however, the growth of $Li_{0.99}Na_{0.01}Nb_{1-y}Ta_yO_3$ films, y = 0.1-, 0.20, 0.30 and 0.40, were successful on the Y-cut $LiTaO_3$ substrate, and films as thick as 15 to 25 μm could easily be grown. The film quality is excellent, and the surface has been found to be relatively smooth enough to fabricate SAW devices on it.

Other charge-coupled substituted systems such as $Li_{1-x}Co_xNb_{1-x}Zr_xO_3$ and $Li_{1-x}Ca_xNb_{1-x}Ti_xO_3$ were studied by using the $LiVO_3$ flux system. Since $CoZrO_3$ and $CaTiO_3$ phases were stable over the $LiNbO_3$, substitution of these ions was found to be difficult in the $LiNbO_3$ films using the $LiVO_3$ flux. In the system $LiVO_3$-$Li_{1-x}Co_xNb_{1-x}Zr_xO_3$, in spite of all these difficulties, we managed to introduce the very small amounts of cobalt and zirconium in the $LiNbO_3$ films. For this small addition, the temperature coefficient of SAW velocity reduced from -90 ppm/°C for $LiNbO_3$ to -79 ppm/°C. We conclude from

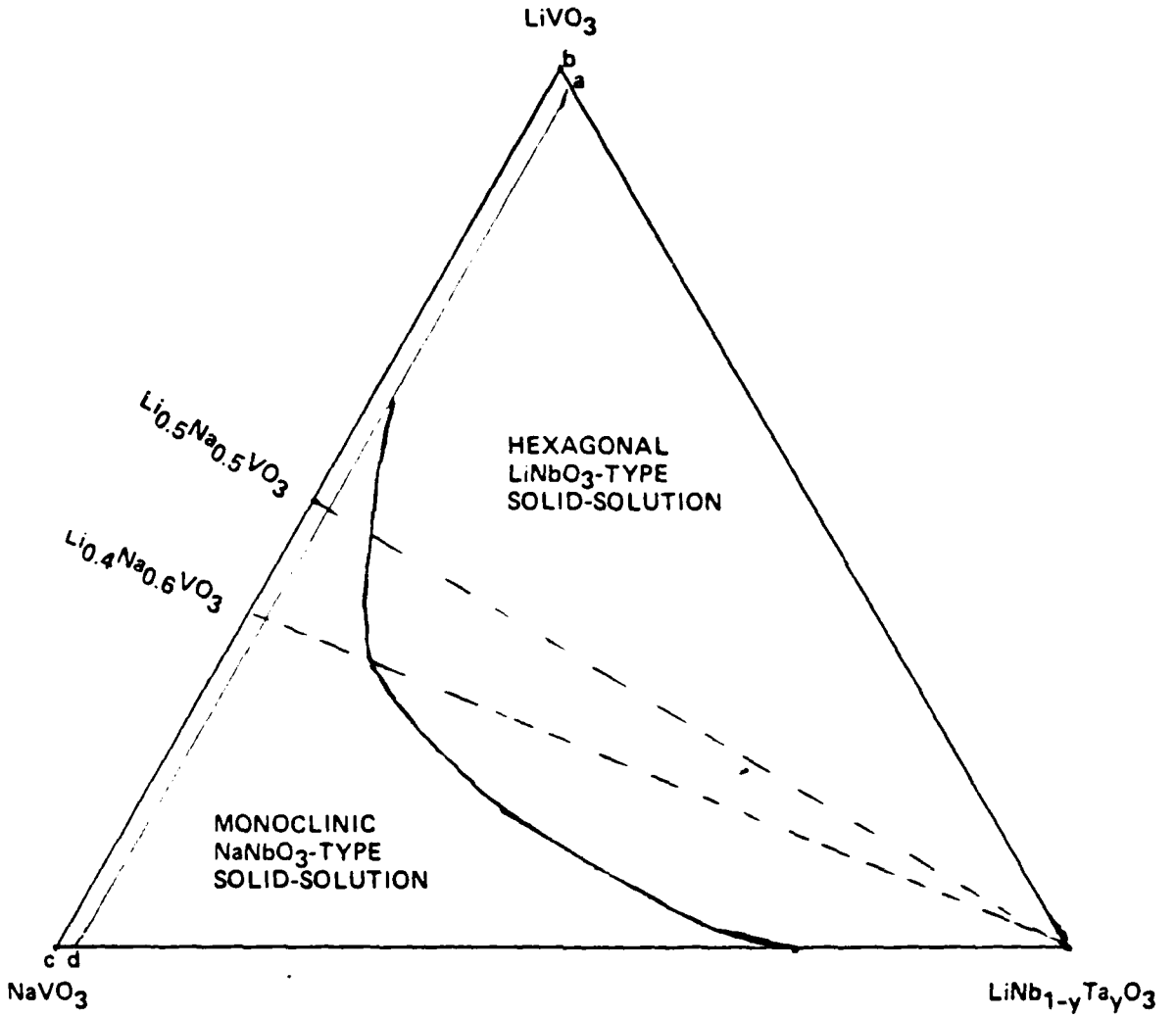

Fig. 6 System $NaVO_3$-$LiVO_3$-$LiNb_{1-y}Ta_yO_3$, in air, at 1250°C.

this results by using proper flux systems, it may be possible to control the concentration of cobalt and zirconium in the $LiNbO_3$ films.

3.5 Thin Film Characterization

The thin films have been characterized by the variety of techniques. Lattice constants and compositional homogeneity was established by the various x-ray powder diffraction techniques. The Laue, Debye-Scherrer and the x-ray topography techniques were also employed to orient and analyze the grown films.

The temperature dependence dielectric properties for the solid solutions and single crystals were established to determine the Curie temperature T_c by the standard process, i.e., measuring the capacitance as a function of temperature in the desired range. The information obtained from this work was necessary in the present work to pole the films to evaluate their acoustical properties.

3.5.1 Crystallinity and Lattice Constants of Thin Films

The crystallinity and the unit cell a_A of the new films and substrate were studied by the x-ray diffraction technique. The Y-cut $LiNbO_3$ substrate showed a reflection corresponding to (300) plane. Figure 7 (a-d) shows the relative intensity of (300) as a function of film thickness. Two peaks corresponding to $CuK_{\alpha 1}$ and $K_{\alpha 2}$ represent the $LiNbO_3$ substrate while the film position is denoted by $CuK'_{\alpha 1}$ and $K'_{\alpha 2}$. The reflection $CuK_{\alpha 1}$ and $K_{\alpha 2}$ of

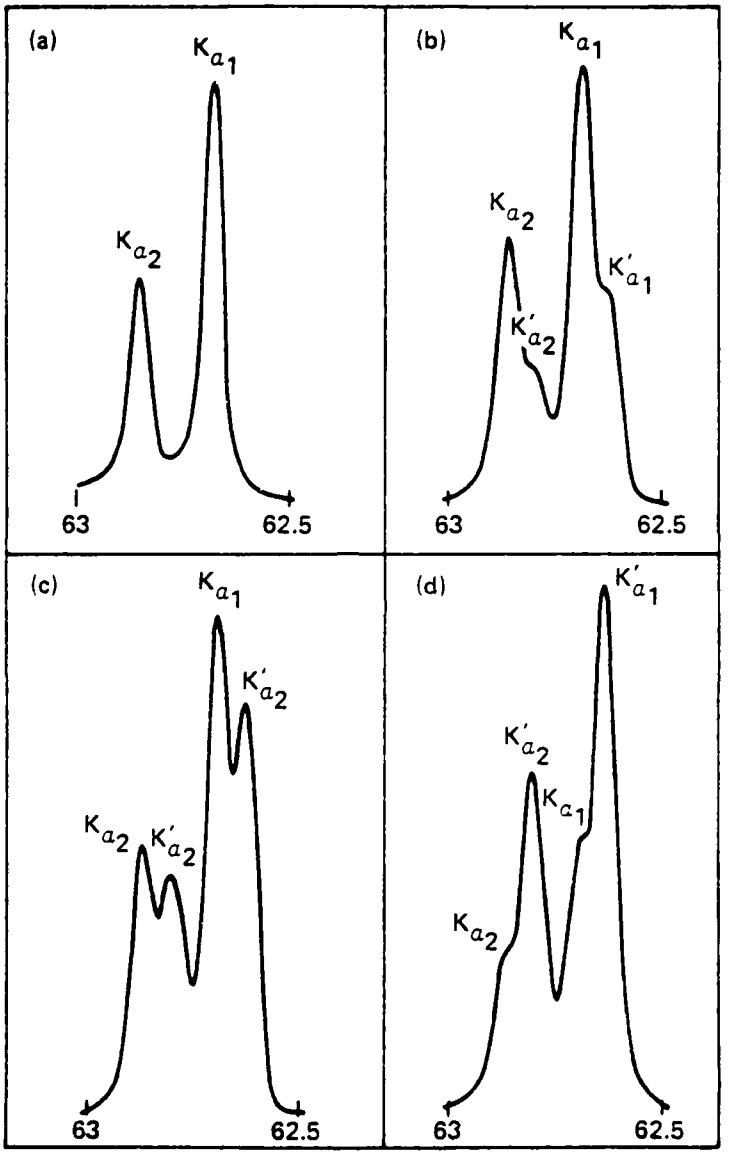

Fig. 7 X-ray diffraction peak (300) taken for substrate/film.

substrate disappeared when 10 μm or thicker films were deposited. The lattice constants for various films were measured using this reflection and they have been summarized in Table 2. Based on this information, it was found possible to establish the relative concentration of each cation in the modified $LiNbO_3$ films.

Table 2

Lattice Constants for Substrate/Film of Modified $LiNbO_3$

Flux	Substrate/Film	Lattice Constants a_A	Lattice Constants c_A	Reference
K_2WO_4	$LiTaO_3$-S	5.152	-	Ballman et al
	$LiNbO_3$-F	5.153	-	(12)
KVO_3	$LiNbO_3$-S	5.148	-	Present Work
	$LiNbO_3$-F	5.152	-	
$LiVO_3$	$LiNbO_3$-S	5.148	-	Present Work
	$LiNbO_3$-F	5.142	-	
$LiVO_3$	$LiTaO_3$-S	-	13.785	Kondo et al
	$LiNbO_3$-F	-	13.870	(15)
$Li_{1-x}NaVO_3$	$LiNbO_3$-S	5.148	-	Present Work
	$Li_{1-x}Na_xNbO_3$-F	5.156	-	
$Li_{1-x}NaVO_3$	$LiTaO_3$-S	5.152	-	Present Work
	$Li_{1-x}Na_xNb_{1-y}Ta_yO_3$-F	5.157	-	
$LiVO_3$	$LiNbO_3$-S	5.148	-	Present Work
	$Li_{1-x}Co_xNb_{1-x}Zr_xO_3$-F	5.147	-	

S = Substrate
F = Film

3.5.2 Temperature Stability of Epitaxial Films

The primary objective of this study is to develop temperature-stable materials for SAW applications. Therefore, the evaluation of temperature

stability is of prime concern. The SAW resonator, as shown in Fig. 8, is ideal for such an investigation. The detailed discussion of such resonators is given by Staples.[21]

To evaluate the temperature stability, a SAW resonator was used. The resonant frequency was monitored while the device was cycled over a prescribed temperature range. Such an experiment gave information on the temperature stability of the epitaxial layers and also revealed any relaxation or internal stresses within the films.

In addition to temperature stability, both short- and long-term stability of the SAW resonators could be investigated. These measurements would yield information regarding aging effects in epitaxial thin film materials.

In these material characterizations, the need for rapid feedback of information to the crystal grower and larger number of measurements required the use of an automated testing procedure. At Rockwell such equipment and system are part of the SAW devices laboratory. The measurement system consists of an HP 8507 network analyzer phase locked to an HP 8660 frequency synthesizer and a Symtek progammable temperature chamber. Each instrument connected by means of an HPIB interface bus is capable of "listening" and "talking" to an HP 9825 calculator. The software of the calculator directs the synthesizer and network analyzer to track zero phase of the SAW resonator at resonance as the tempeature is varied. In this arrangement, computation, formulation and plotting of the data takes place as it is measured. By

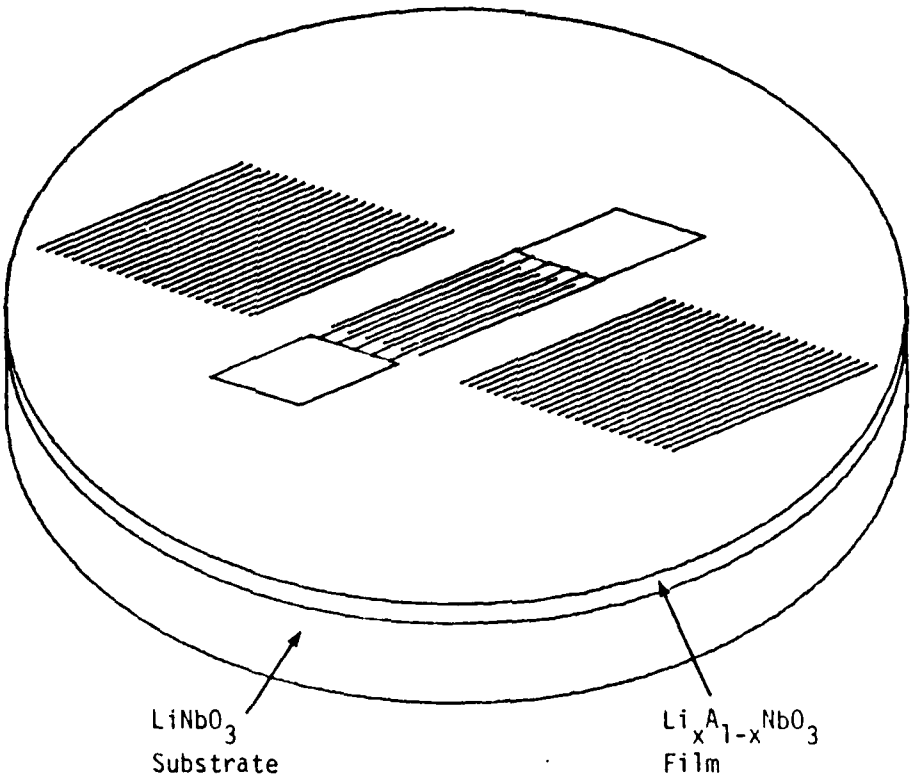

Fig. 8 Configuration of SAW resonator.

utilizing this unique measurement system, the processed data can quickly be analyzed and rapid feedback of information is assured.

The temperature coefficient of SAW velocity was determined for various films containing Na^+, Co^{2+} + Cr^{4+}, Na^+ + Ta^{5+}, etc. Approximately 20 to 30 μm thick films were used and the measurements were accomplished as described above. This coefficient was first established for pure $LiNbO_3$ films and was found to be -88 ppm/°C. This measured value is in excellent agreement with the value, -90 ppm/°C reported for single crystals of $LiNbO_3$. As shown in Fig. 9, this value dropped to -56 ppm/°C for $Li_{0.99}Na_{0.01}NbO_3$ films. These results are reproducible and indicate that the crystal chemistry approach is successful in the present case. This is a significant accomplishment and opens a new interest in the surface acoustic wave device area; it also suggests that by using higher concentation of Na^+ in the films, it should be possible to control this coefficient to the desired temperature range. Although there is an excellent opportunity in the present work to achieve the proposed goal, the growth was found to be difficult due to large mismatching between $Li_{0.97}Na_{0.03}NbO_3$ on the $LiNbO_3$ substrate. It seems logical that by exploring a suitable substrate material for this growth, it should be possible in the future to continue this work.

Co^{2+} + Zr^{4+} and Nb^{5+}-rich $LiNbO_3$ were also studied, and it was found that the temperature coefficient of SAW velocity reduced for the cobalt and zirconium modified $LiNbO_3$ films (-79 ppm/°C), indicating the possible inclusion of cobalt and zirconium in the films. In case of Nb^{5+}-rich films, the measurements were found to be inconsistent and inconclusive. This

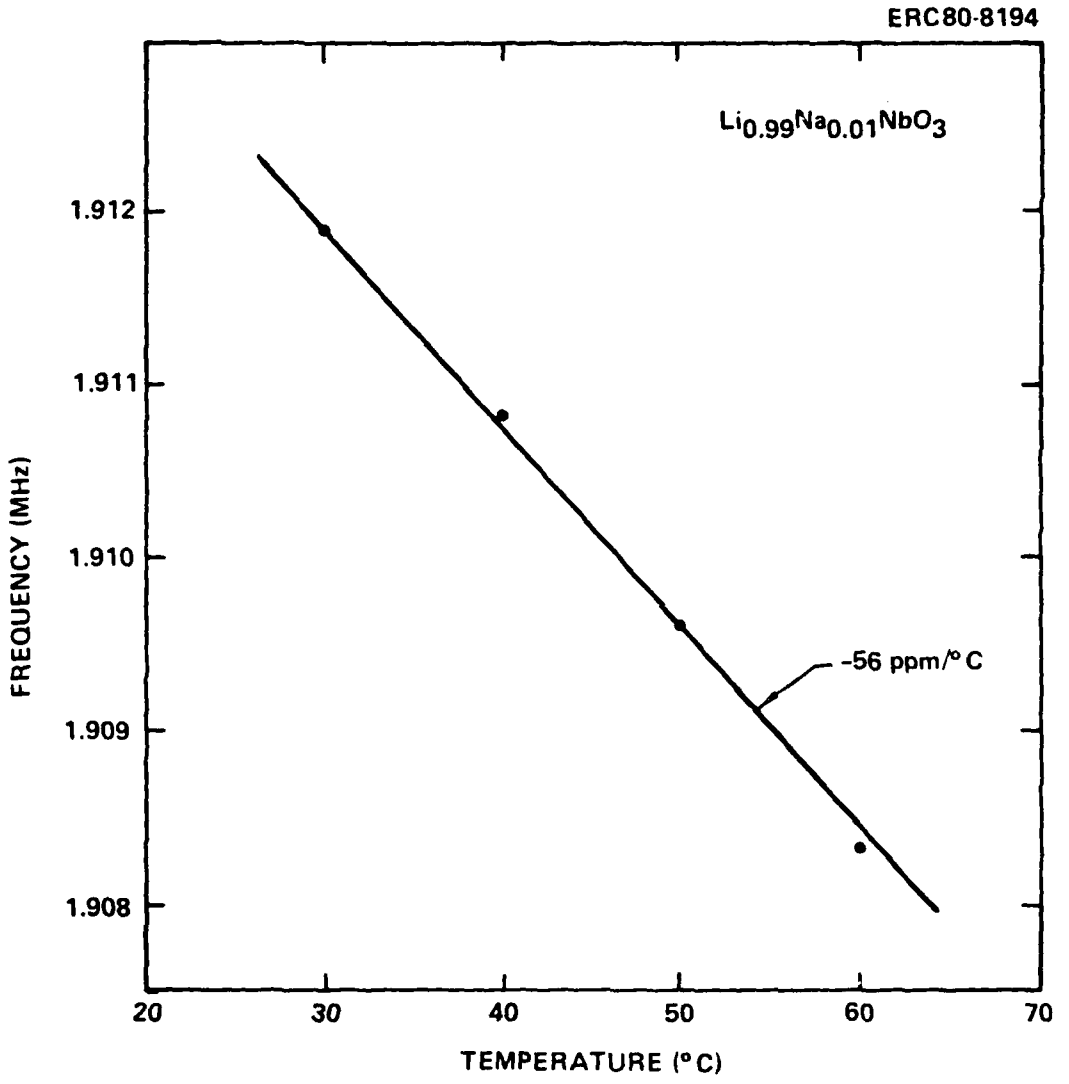

Fig. 9 Frequency as a function of temperature for $Li_{0.99}Na_{0.1}NbO_3$ films on the Y-cut $LiNbO_3$ substrate.

strongly suggests that since the films were grown near the Curie temperature of $LiNbO_3$ (1200°C), the substrate and films must have depoled. The $Li_{0.99}Na_{0.01}Nb_{1-y}Ta_yO_3$ films were also evaluated. In this case, films had to be poled since they were grown on the $LiTaO_3$ substrate. $LiTaO_3$ has a Curie temperature around 660°C, and it was found diffucult to pole. Because the poling technique is not well established for thin film area, this seems to be significantly important in future work.

Figure 10 shows frequency response of this device. The insertion loss for the $Li_{0.99}Na_{0.01}NbO_3$ films is about -24 dB. For comparison, using the same mask on pure $LiNbO_3$ films, an insertion loss of about -22 dB was observed. This result indicates that the electromechanical coupling constant (K^2) remained unchanged for the sodium modified $LiNbO_3$ films. This is also a significant result of this work.

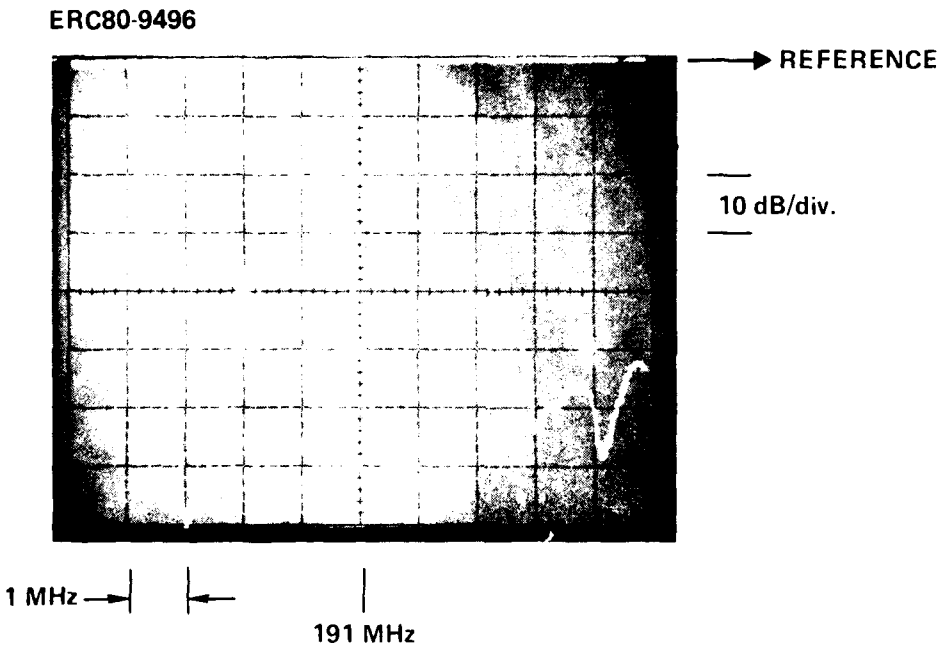

Fig. 10 Frequency response of SAW filter on $Li_{0.99}Na_{0.1}NbO_3$ film.

4.0 CRYSTAL CHEMISTRY

4.1 Limits of Stability of the $LiNbO_3$-Structure

The limits of stability of the $LiNbO_3$-structure was established by introducing various ions for the Li^+ and Nb^{5+} or Ta^{5+} positions. The substitutions were made as follows:

1. $LiM^{5+}O_3 + M^{2+}M^{4+}O_3 \rightarrow Li_{1-x}M^{2}_{x}M^{5}_{1-x}M^{4}_{x}O_3$

   where M^{2+} → Ca, Cd, Co, or Mg

   M^{5+} → Ta or Nb

   M^{4+} → Zr, Ti, or Sn

2. $LiM^{5+}O_3 + M^{+}M^{5+}O_3 \rightarrow Li_{1-x}M^{+}_{x}M^{5+}O_3$

   where M^{+} → Na, Ag, or K

3. $LiM^{5+}O_3 + M^{3+}M^{3+}O_3 \rightarrow Li_{1-x}M^{3+}_{x}M^{5+}_{1-x}M^{3+}_{x}O_3$

   where M^{3+} → Ga, In, Y, Eu

All the phases have been synthesized by the solid state technique, using analytical grade starting materials. After calcining around 700-800°C for 20 hours, each batch mixture was ball-milled in acetone for 3-4 hours,

dried and pressed into disks. The pressed disks, except Ag^+ containing niobates or tantalates, have been fired at 1100-1360°C for 4-6 hours. Since Ag^+ volatilizes above 1100°C, all $Li_{1-x}Ag_xM^{5+}O_3$ compositions have been heat-treated at approximately 1100°C. The x-ray powder diffraction technique has been used to identify phase purity, and to determine the lattice constants for the different ilmenite solid-solution systems.

Table 3 summarizes the exprimental conditions, the limits of solid-solubility range of substitutional ions and the changes in the unit cell volume for different solid solution systems.

Figure 11 shows the structure field map for the $LiNbO_3$-type solid solutions. The radii (Shannon and Prewitt) of ions occupying the Li^+ and Nb^{5+} or Ta^{5+} positions in the $LiNbO_3$-structure are plotted along the ordinate and abscissa respectively. The diagram has been divided into different parts according to the extent of solid solubility of substitutional ions. A complete solid-solubility has been reported[19,20] for the $LiNbO_3$-$LiTaO_3$ system. All other substitutions are partial in the $LiM^{5+}O_3$ phase. $M^{2+}TiO_3$, M = Cd, Zn, Co, Ni or Mg, belong to the ilmenite structural family and are structurally similar to the $LiNbO_3$ structure. Both $M^{2+}TiO_3$ and $LiM^{5+}O_3$ dissolve mutually to a large extent without changing crystal symmetry. The ilmenite solid solution $Li_{1-x}Cd_xM^{5+}_{1-x}Ti_xO_3$, where $0.70 > X < 1.0$ exhibited the ilmenite-perovskite structural transition around 1100°C. The samples on the $Li_{1-x}Zn_xM^{5+}_{1-x}Ti_xO_3$ system were difficult to prepare since the ilmenite $ZnTiO_3$ converts to α - Zn_2TiO_4 at 700°C.

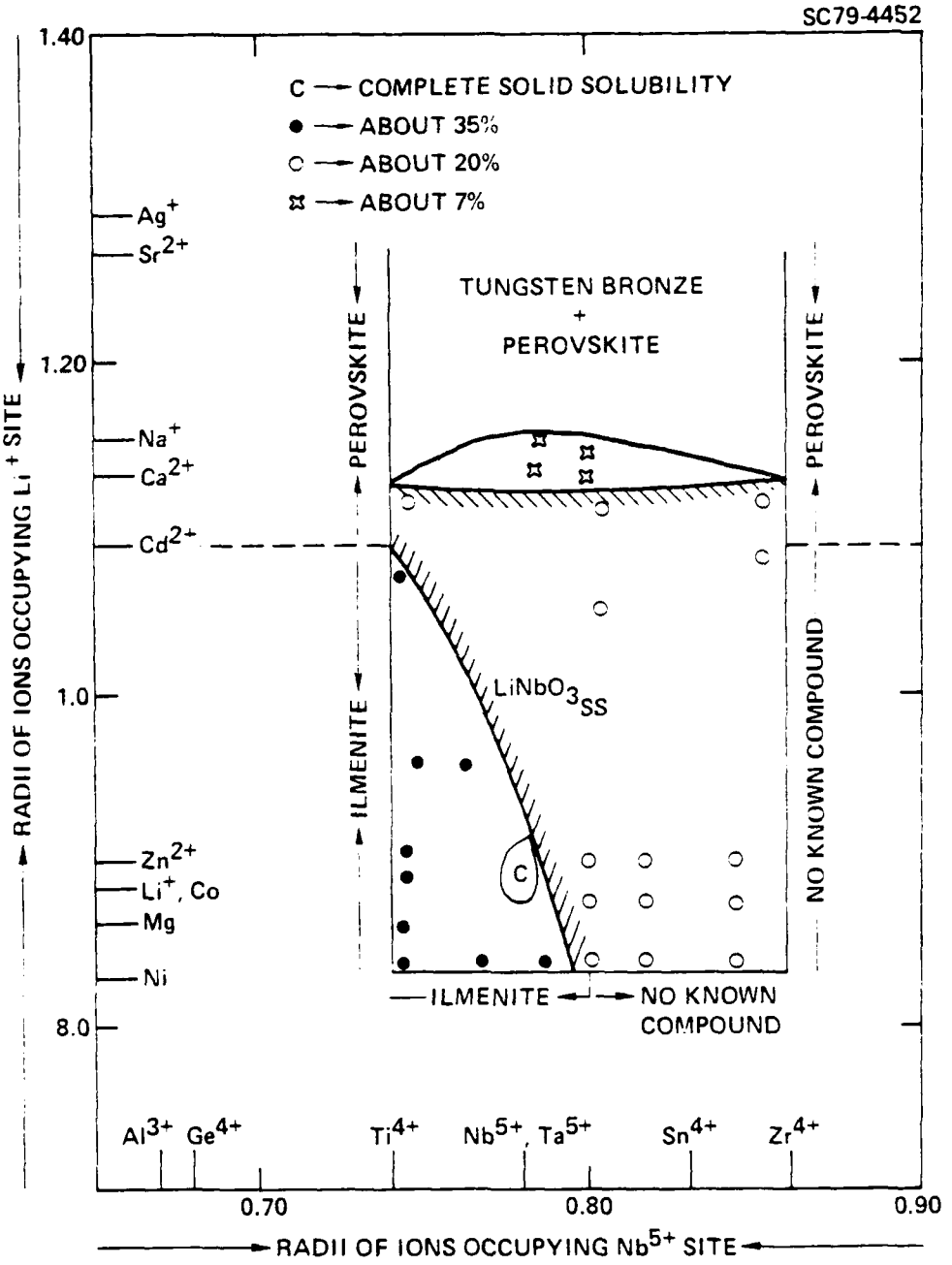

Fig. 11 The structural field map for the $LiNbO_3$ solid solutions.

Table 3

Crystalline Solubility of Various Ions in $LiM^{5+}O_3$, M = Nb or Ta

System	Firing Temp (°C)	Range of $LiNbO_3$ Structure	Structural Change	Unit Cell Volume	Reference
$LiM^{5+}O_3$-$M^{2+}TiO_3$ M^{2+} = Cd, Zn, Co, Ni or Mg	1000-1300	~ 30-35%	None	Decreases*	Present Work
$LiM^{5+}O_3$-$M^{2+}M^{4+}O_3$ M^{2+} = Ca, Cd, Co, M^{4+} = Zr or Sn	1200-1400	~ 20%	One Change - On $Li_{1-x}Ca_xTa_{1-x}Zr_xO_3$	Increases	Present Work
$LiM^{5+}O_3$-$M^{+}M^{5+}O_3$ M^{+} = Ag or Na	1000-1100	~ 7%	Change at the $M^{+}M^{5+}O_3$ End	Increases	Present Work
$LiM^{5+}O_3$-$M^{3+}M^{3+}O_3$	1000-1300	< 2%	---	---	Present Work

*Except for $CdTiO_3$

Approximately 20 mole% $M^{2+}SnO_3$ and $M^{2+}ZrO_3$, where M = Ca, Cd, Co or Mg, dissolve in the $LiM^{5+}O_3$ phase. A notable feature in this series is occurance of a structurally new phase on the $Li_{1-x}Ca_xTa_{1-x}Zr_xO_3$ system.[22] This structural change can be discussed on the basis of the ions that are replacing Ta^{5+}. Zr^{4+} (0.86 Å) is substantially bigger than Ti^{4+} (0.74 Å), and further there is no $M^{2+}ZrO_3$ analog to the ilmenite structure compounds $M^{2+}TiO_3$, M = Cd, Zn, Co, Ni or Mg. This strongly suggests that Zr^{4+} is a bigger ion to accommodate into the ilmenite-structure. This could be an appropriate reason why the ilmenite symmetry changed for the higher concentrations of $CaZrO_3$.

The solid solubility of $NaM^{5+}O_3$ and $AgM^{5+}O_3$, M = Nb or Ta, was found to be limited to 7 mole% in $LiM^{5+}O_3$.[17] At the other end the perovskite solid solution $Li_{1-x}M^{+}_xM^{5+}O_3$, $0.85 > X < 1.0$ showed three structural changes as seen for the pure $NaNbO_3$ and $AgNbO_3$ phases. The substitution of Al^{3+}, Fe^{3+}, In^{3+}, Y^{3+} or Gd^{3+} for the Li^+ or Nb^{5+} positions was unsuccessful.

Based on these observations, one could generalize the results of the present study as follows:

1. The size of substitutional ions should be close to Li^+ and Nb^{5+}, e.g., a complete solid solution in the system $LiNbO_3$ - $LiTaO_3$.

2. The substitutions should be made on both the Li and Nb positions, e.g., the higher solid solubility in the systems $LiM^{5+}O_3$ - $M^{2+}M^{4+}O_3$.

3. Valance state of substitutional ions should be low, e.g., unsuccessful substitution of Al^{3+}, Fe^{3+}, In^{3+} or Y^{3+} in $LiM^{5+}O_3$.

4.2 Lattice Constants for the $LiNbO_3$-Solid-Solutions

Lattice constants for a_A and c_A for the ilmenite solid solutions have been accurately determined by the x-ray powder diffraction technique (scanning 1/2°, 2θ/min) and using silicon as an internal standard. Using a least-squares computer program, the lattice constants were refined. Figure 12 shows the variation of a_A and c_A for different solid-solutions. The lower box in Fig. 12 represents the changes in lattice constant a_A while the changes in lattice constant c_A are given in the upper box. The results of this study indicate that the lattice constants a_A increased while c_A decreased for the ions bigger than Li^+ and Nb^{5+}, i.e., the phases contained ions like Ca^{2+}, Cd^{2+}, Na^+ and Zr^{4+}. On the other hand, the lattice constants a_A decreased while c_A increased for the ions smaller than Li^+ and Ta^{5+} or Nb^{5+}, i.e., for Mg^{2+}, Ti^{4+}, etc. The lattice constants for the substituted $LiNbO_3$ have also been calculated and have similar changes as seen for the $LiTaO_3$. Hence, they are not duplicated here.

4.3 Dielectric Data

The Curie temperature T_c is known to be one of the fundamental characteristics of ferro- and antiferroelectrics. this measurement gives the origin of the spontaneously polarized state and is considered important for characterizing the piezoelectric materials. In the present work, the T_c for

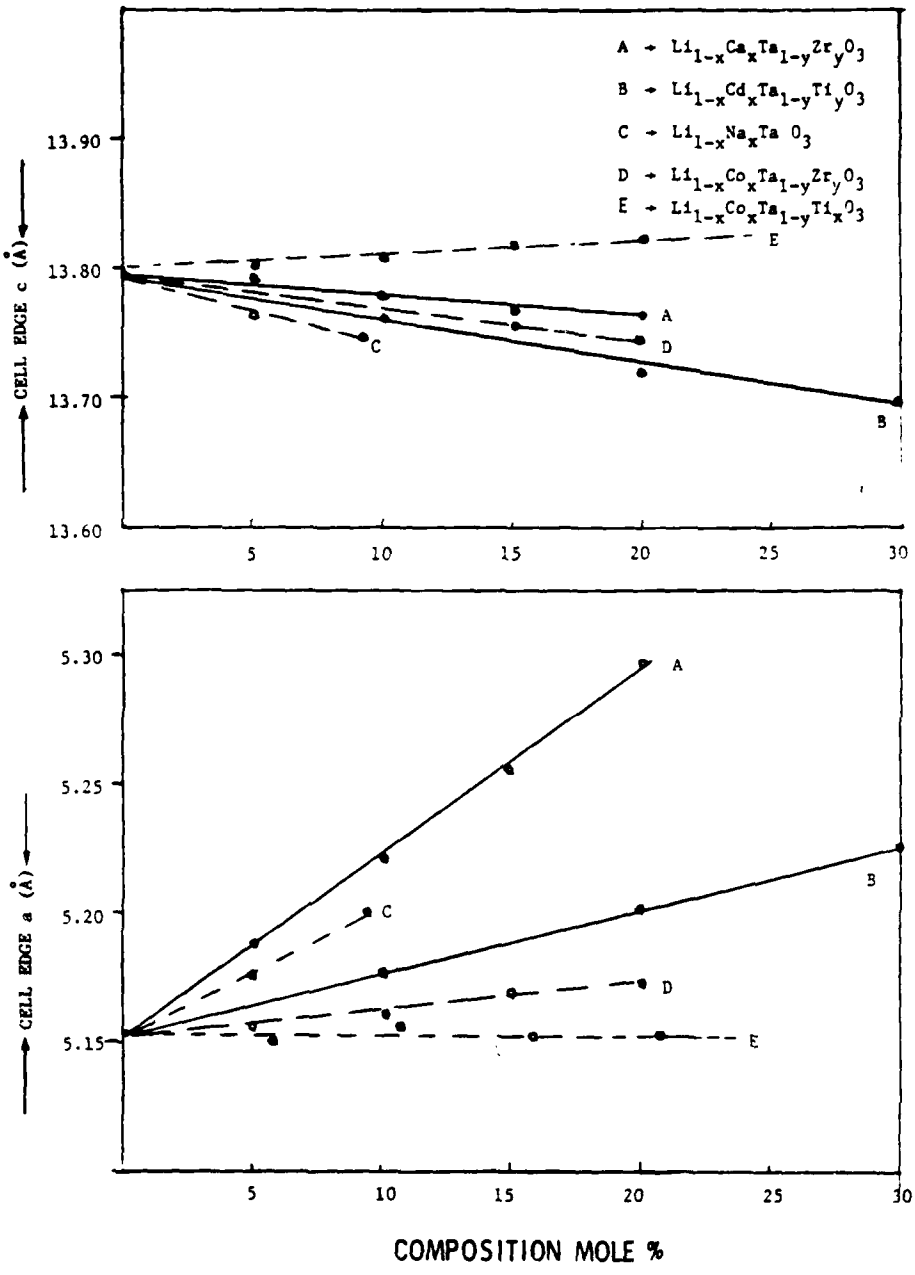

Fig. 12 Lattice constants for the ilmenite solid solution systems.

the different solid-solution systems has been obtained by measuring the dielectric properties as a function of temperature. The technique is relatively simple and the measurements are made routinely using a capacitance bridge (HP 4270A). The test specimens (disks) used for the dielectric measurements are approximately 1.3 cm in diameter and 0.3 cm thick, and coated on each side with platinum by the standard vacuum evaporation technique.

A typical plot of the dielectric constant vs temperature is given in Fig. 13 for the two end member conpositions, $LiTaO_3$ and $Li_{1-x}Ca_xTa_{1-x}Zr_xO_3$. It can be seen that the peak at Curie temperature is sharp and is shifted towards a lower temperature with the addition of 20 mole% $CaZrO_3$ in $LiTaO_3$. The T_c for the pure $LiTaO_3$ and $LiNbO_3$ was recorded at 670°C and 1170°C, which are in good agreement with results reported for the polycrystalline phases in the literature.[23] Using this peak position, the transition temperature for each sample has been determined. Figure 14 shows the variation of the T_c as a function of composition for the $Li_{1-x}Ca_xTa_{1-x}Zr_xO_3$ and the various other systems. The results of this study show that the T_c decreases for the ilmenite solid solutions with increased concentrations of $CaZrO_3$, $CdTiO_3$ $NaTaO_3$, or $CoZrO_3$ in $LiTaO_3$ or $LiNbO_3$. On the other hand, the addition of $MgTiO_3$ or $CoTiO_3$ shifts the T_c towards a higher temperature.

It is clear from these results that the decrease in T_c for the ilmenite solid-solution can be related to the fact that the volume of the hexagonal unit cell increases by the addition of bigger cations such as Ca^{2+} (1.14 A), Cd^{2+} (1.09 A), Na^+ (1.16 A), and Zr^{4+} (0.86 A), for Li^+ (0.88 A), and Nb^{5+} or Ta^{5+} (0.78 A). The systems $LiM^{5+}O_3$ - $CdTiO_3$[24] and $LiTaO_3$ -

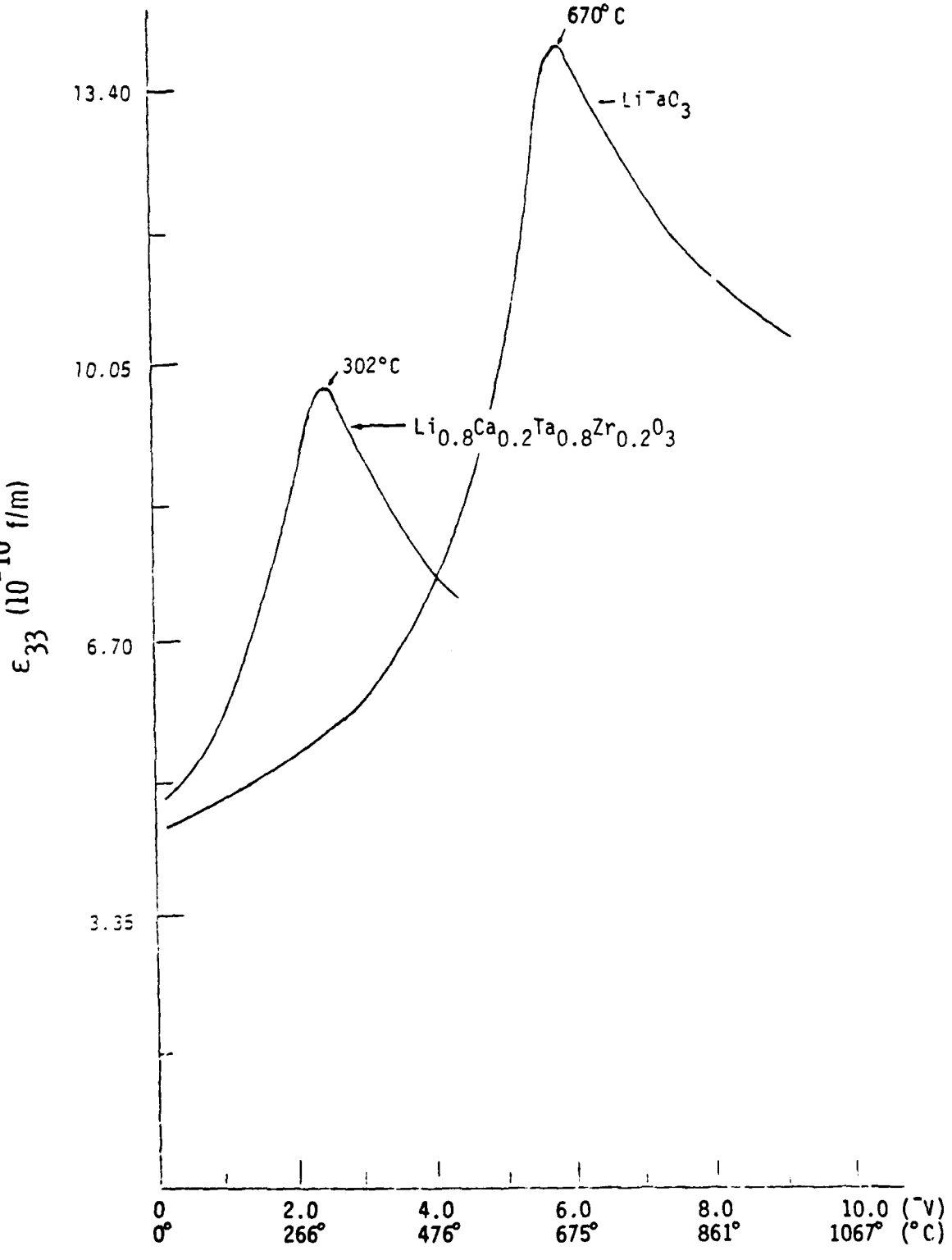

Fig. 13 Curie temperature for $LiM^{5+}O_3$-$CaZrO_3$ system.

A^1 — $Li_{1-x}Cd_xNb_{1-y}Ti_yO_3$

B^1 — $Li_{1-x}Ca_xNb_{1-y}Zr_yO_3$

A — $Li_{1-x}Ca_xTa_{1-y}Zr_yO_3$

B — $Li_{1-x}Ca_xTa_{1-y}Ti_yO_3$

C — $Li_{1-x}Na_xTaO_3$

D — $Li_{1-x}Co_xTa_{1-y}Ti_yO_3$

E — $Li_{1-x}Mg_xTa_{1-y}Ti_yO_3$

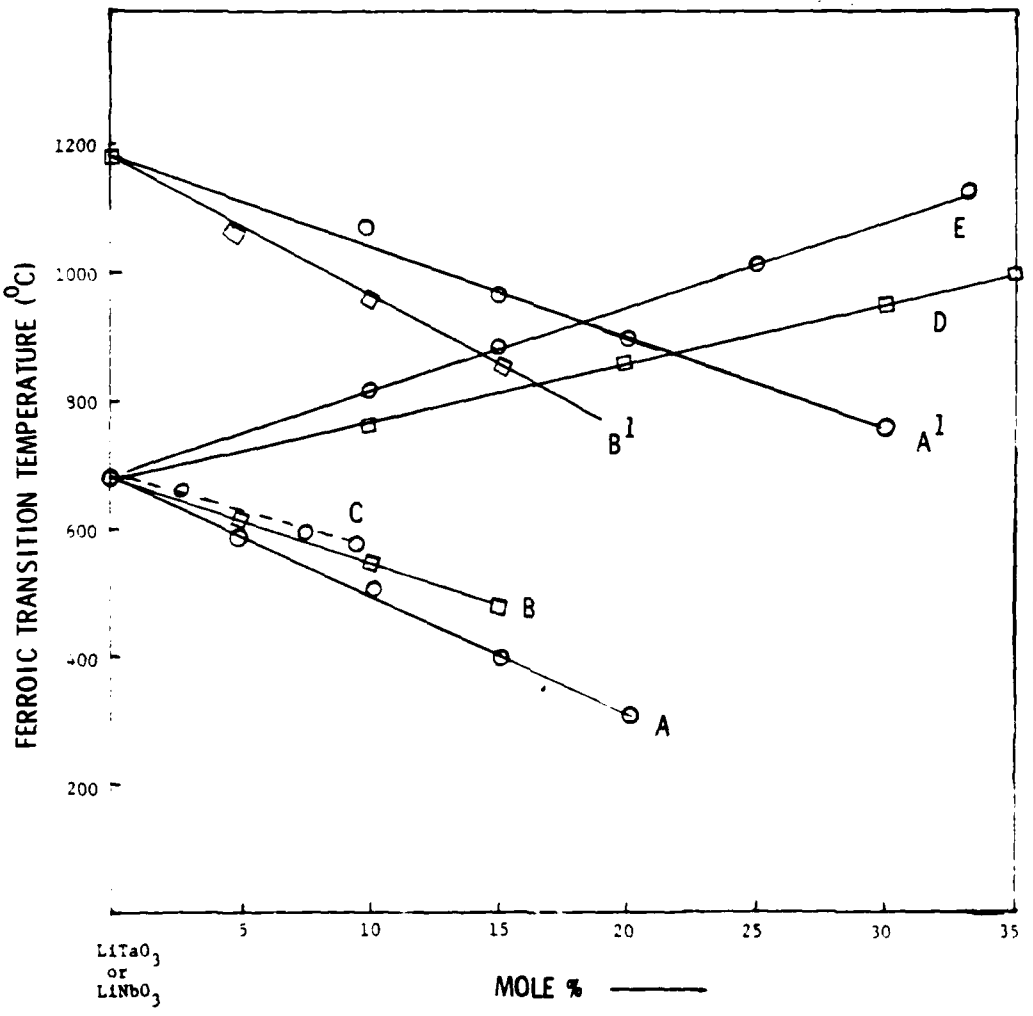

Fig. 14 Ferroic transition temperature vs composition.

$NaTaO_3$[25] have previously been studied and the results of this work are in good agreement with the reported work. Both Mg^{2+} (0.86 Å) and Ti^{4+} (0.74 Å) are smaller than Li^+ and M^{5+}, and hence, reduce the unit cell colume and shift the T_c towards a higher temperature. Figure 15 summarizes the T_c changes for the entire $LiM^{5+}O_3$ - $M^{2+}M^{4+}O_3$ and $LiM^{5+}O_3$ - $M^{+}M^{5+}O_3$ systems. The results are grouped into two categories according to the variation of the T_c with respect to the given cations in the different systems.

In summary, the cations with bigger ionic radii than Li^+ and Ta^{5+} or Nb^{5+} would shift the T_c towards a lower temperature and vice versa.

VARIATION OF THE FERROIC TRANSITION TEMPERATURE FOR THE DOPED $LiM^{5+}O_3$ SYSTEM, M = NbOrTa

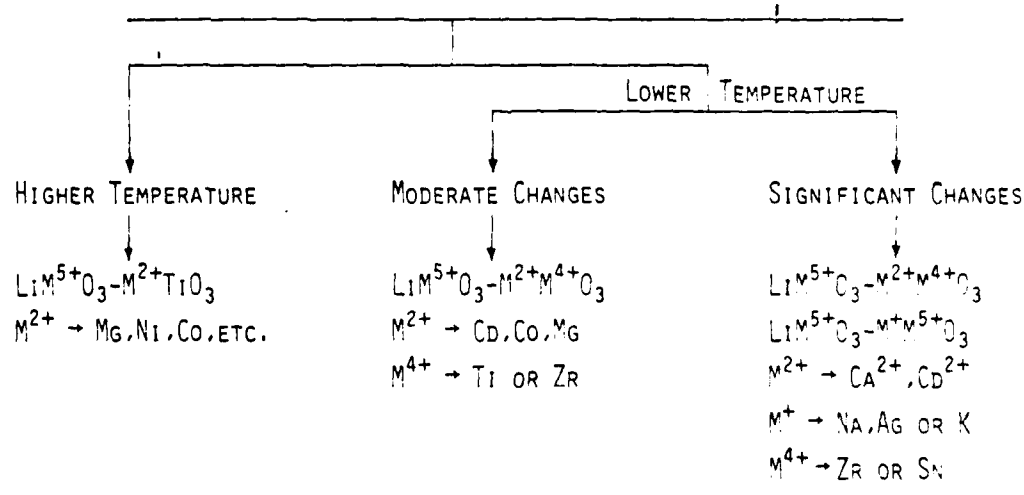

Conclusions

Lower Temperature:

1. Higher temperature: both cations smaller than Li^+ and M^{5+}
2. Moderate changes
   - A. One cation significantly bigger than Li^+; other smaller than M^{5+}, or
   - B. Both cations slightly bigger than Li^+ and M^{5+}
3. Significant change
   - A. Both cations are substantially bigger than Li^+ and M^{5+}
   - B. One cation significantly bigger than Li^+ without changing other cation M^{5+}

Fig. 15 Variation of the ferroic transition temperature for the doped $LiM^{5+}O_3$, M = Nb or Ta.

5.0 CONCLUSIONS AND REMARKS

The goal of this research was to demonstrate the feasibility of modified $LiNbO_3$ thin films for surface acoustic wave device application. This is the first time such a technique is being developed and exploited for surface acoustic wave applications. The program included the growth of single crystalline modified $LiNbO_3$ thin films by the liquid phase epitaxial growth technique and evaluation of their structural and acoustical properties. The crystal chemical role of various ions in the $LiNbO_3$-structure was also established.

Throughout this study, we have noted a striking similarity between our work and the use of thin film magnetic garnet films grown on single crystal garnet substrates by the LPE technique for magnetic bubble applications. The choice of substrate and film are known to depend on several considerations, e.g., they should be of the same crystal class and have similar lattice match, and the temperature coefficient of linear expansion should be the same and be easily prepared under the crystalline purity. In the work reported here, $LiNbO_3$ satisfied these requirements and is available in 2 in. diameter boules, which are defect-free and can be polished into slices of the crystal purity and surface finish necessary for epitaxial depositions.

Our success in developing Na^+-modified $LiNbO_3$ films indicate that the LPE technique can effectively be employed in surface acoustic wave technology to improve their properties. The results of the present investigation

indicate that the addition of 1 mole% sodium in the $LiNbO_3$ films reduced the temperature coefficient of surface acoustic wave velocity from -90 ppm/°C for pure $LiNbO_3$ to -56 ppm°C for the $Li_{0.99}Na_{0.01}NbO_3$ thin films. The improvement is almost 40%; this indicates that this coefficient can be reduced further if more sodium is incorporated in the $LiNbO_3$ films. Although, this presents an excellent opportunity to developed modified $LiNbO_3$ thin films with high coupling constants (SAW coupling K^2) and sufficiently low temperature coefficient of surface acoustic wave velocity, the growth of highly concentrated Na^+-modified films (above 2 mole%) was not achieved because of a lack of suitable substrate materials.

In summary, the LPE growth technique to grow modified $LiNbO_3$ thin films of desired compositions and specifications has been shown to be successful, and there is a significant improvement in the temperature stability of the $LiNbO_3$ phase. Since $LiNbO_3$ is one of the most interesting ferroelectric materials for piezoelectric and optical applications such as electro-optic, acousto-optic, and non-linear optics, the new improved modified $LiNbO_3$ should prove to be useful for these applications. We believe, this new improved $LiNbO_3$ SAW filters or as optical material will produce significant impact as important elements in such DoD systems such as radar, communication, and navigation equipments.

6.0 REFERENCES

1. S.I. Long, J.M. Ballantyne and L.F. Eastman, "Steady-State LPE Growth of GaAs," J. Cryst. Growth 26, 13 (1974).

2. R.L. Moon and J. Kinoshita, "Comparison of Theory and Experiments for LPE Layer Thickness of GaAs and GaAs Alloys," J. Cryst. Growth 21, 149 (1974).

3. S.Y Lien and J.L. Bestel, "LPE Growth of GaP by a Centrifugal Tipping Technique," J. Electrochem. Soc. 120, 1571 (1973).

4. D.L. Rode, "Isothermal Diffusion Theory of LPE: GaAs, GaP, Bubble Garnet," J. Cryst. Growth 20, 13 (1973).

5. H. Kressel, "GaAs and (AlGa)As Devices Prepared by LPE," J. Electronic Materials 3, 747 (1974).

6. M. Nakamura, K. Aiki, J. Umeda, A. Yariv, H.W. Yien and T. Morikawa, "LPE of GaAlAs on GaAs Substrates with Fine Surface Corrugations," Appl. Phys. Lett. 24, 466 (1974).

7. A.A. Barsh, R.H. Saul and C.R. Paola, "Growth of GaP Layers from Thin Aliquot Melts: LPE as a Commercial Process," J. Electrochem. Soc. 120, 1558 (1973).

8. H.J. Levingstein, S. Licht, R.W. Landorf and S.L. Bank, "Growth of High Quality Garnet Thin Films from Supercooled Melts," Appl. Phys. Lett. 19, 486 (1971).

9. L. Ghes and E.A. Geiss, "Temperature Dependence of Garnet LPE Growth Kinetics," J. Cryst. Growth 27, 221 (1974).

10. T. Kasai, Z. Tajma and T. Ikeda, "Control of the Anisotropy Field of Successively Grown Garnet Films," Mat. Res. Bull. 12, 503 (1977).

11. H.L. Glass, J.H.W. Liaw and M.T. Elliott, "Temperature Stabilization of Ferromagnetic Resonance Field in Epitaxial YIG by Ga and La Substitution," Mat. Res. Bull. 735 (1977).

12. A.A. Ballman, H. Brown, P.K. Tien and S. Riva-Sanseverino, "The Growth of $LiNbO_3$ Thin Films by LPE Techniques," J. Cryst. Growth 29, 298 (1975).

13. A Baudrant, H. Vial and J. Davel, "LPE of $LiNbO_3$ Thin Films for Integrated Optics," Mat. Res. Bull. 10, 1373 (1975).

14. S. Miyazawa, "Growth of $LiNbO_3$ Single Crystal Film for Optical Wave Guides," Appl. Phys. Lett. 23, 198 (1973).

15. S. Kondo, S. Miyazawa, S. Fushimi and K. Sugi, "LPE Growth of Single Crystal $LiNbO_3$ Thin Films," Appl. Phys. Lett. 26, 489 (1975).

16. R.R. Neurgaonkar, T.C. Lim and E.J. Staples, "Structural and Dielectric Properties in the System $LiTaO_3$ - $CaZrO^4$," Mat. Res. Bull.

17. J. LaComte and E. Quemeneux, Contribution a' l'etude Structurale des Composes $Na_{1-x}Li_xNbO_3$, Bull. De. La. Societe Chimique de France 12, 2779 (1974).

18. R.R. Neurgaonkar, T.C. Lim, E.J. Staples and L.E. Cross, "An Exploration of the Limits of Stability of the $LiNbO_3$ Structure Field with A and B Cation Substitutions," Ferroelectrics, 27-28, 63, 1980.

19. G.E. Peterson, P.M. Bridenbaugh and P. Green, "NMR Study of Ferroelectric $LiNbO_3$ and $LiTaO_3$, I," J. Chem. Phys. 46, 4009 (1967).

20. G.E. Peterson, J.R. Carruthrs and A. Carnevale, "Nb, NMR Study of the $LiNbO_3$- $LiTaO_3$ Solid Solution System," J. Chem. Phys. 53, 2436 (1971).

21. E.J. Staples, "UHF Surface Acoustic Wave Resonators," Proceedings of the 28th Annual Frequency Control Symposium, 280-285, 1979.

22. R.R. Neurgaonkar, T.C. Lim and E.J. Staples, "Structural and Dielectric Properties in the System $LiTaO_3$-$CaZrO_3$," Mat. Res. Bull. 13, 635, 1978.

23. A.A. Ballman, H.J. Levinstein, C.D. Capio and H. Brown, "Curie Temperature and Birefringence Variation in Ferroelectric $LiTaO_3$ as Function of Melt Stoichiometry," J. Am. Chem. Soc. 50, 657 (1967).

24. E.I. Shapiro, "Investigations of the Structure and Dielectric Properties of Solid Solutions in the $LiTaO_3$ - $CdTiO_3$ and $LiNbO_3$ - $CdTiO_3$ Systems," IZV, Akad. Nauk. USSR 3, 2245 (1967).

25. M.M. Sergemetayer, R.V. Muhll, J. Ravez and P. Hagenmuller, "Influence De. La. Substitution Sodium Lithium Surles Properties Crystellographiques etc. Dielectricques De $LiTaO_3$," C.R. Acad. Sc. Paris, t. 282, 799 (1976).

7.0 PUBLICATIONS FROM CURRENT RESEARCH

1. E.J. Staples, R.R. Neurgaonkar and T.C. Lim, "Temperature Coefficient of SAW Velocity on Epitaxial $Li_{1-x}Na_xNbO_3$ Thin Films," Appl. Phys. Lett. 32, 197, 1978.

2. R.R. Neurgaonkar, T.C. Lim and E.J. Staples, "Structural and Dielectric Properties in the System $LiTaO_3$-$CaZrO_3$," Mat. Res. Bull. 13, 635, 1978.

3. R.R. Neurgaonkar, M.H. Kalisher, E.J. Staples and T.C. Lim, "Na^+ and Co^{2+} + Zr^{4+} Doped $LiNbO_3$ Thin Films for SAW Device Applications," Proc. Ultrasonics Symposium, 598, 1979.

4. R.R. Neurgaonkar, M.H. Kalisher, E.J. Staples and T.C. Lim, "Liquid Phase Epitaxy Growth of Na^+ and Co^{2+} + Zr^{4+} Doped $LiNbO_3$ Thin Films," Appl. Phys. Lett. 35, 606, 1979.

5. R.R. Neurgaonkar, T.C. Lim, E.J. Staples and L.E. Cross, "An Exploration of the Limits of Stability of the $LiNbO_3$ Structure Field with A and B Site Cation Substitutions," Ferroelectrics, 27-28 63, 1980.

6. R.R. Neurgaonkar, T.C. Lim, E.J. Staples and L.E. Cross, "Crystal Chemistry of Ferroelectric Materials for SAW Device Applications," Proc. of Ultra-Sonics Symposium, 410, 1980.

7. R.R. Neurgaonkar and E.J. Staples, "Liquid Phase Epitaxial Growth of $LiNbO_3$ Films Grown from $Li_{1-x}Na_xVO_3$ Flux," Accepted J. Crystal Growth.

8. R.R. Neurgaonkar, "Limit of Stability of $LiNbO_3$-Structure," Submitted to Mat. Res. Bull.

Papers Presented at Meetings:

1. R.R. Neurgaonkar, T.C. Lim and E.J. Staples, "Structural and Dielectrical Properties in the Systems $LiM^{5+}O_3$ - $M^{2+}M^{4+}O_3$ and $LiM^{5+}O_3$ - $M^{+}M^{5+}O_3$," presented at the fall meeting of the American Ceramic Society, September 18-20, 1978, Dallas, Texas.

2. R.R. Neurgaonkar, T.C. Lim, E.J. Staples and L.E. Cross, "An Exploration of the Limits of Stability f the $LiNbO_3$ Structure Field and A and B Site Cation Substitutions," to be presented at the IEEE International Symposium of Ferroelectrics, June 13-15, 1979, Minneapolis, Minnesota.

3. R.R. Neurgaonkar, M.H. Kalisher, E.J. Staples and T.C. Lim, "Na^{+} and Co^{2+} + Zr^{4+} Doped $LiNbO_3$ Thin Films for SAW Device Application," presented at the International Ultrasonics Symposium, September 26-28, 1979, New Orleans, Louisiana.

4. R.R. Neurgaonkar, T.C. Lim, E.J. Staples and L.E. Cross, "Crystal Chemistry of Ferroelectric Materials for SAW Device Applications," presented at the International Ultrasonics Symposium, November 1980, Boston, Massachusetts.


ATE
LME